

An Electrospray Ionization–Flow Tube Study of H/D Exchange in Protonated Bradykinin[†]Elchanan Levy-Seri, Grielof Koster,[‡] Alexandra Kogan, Karnit Gutman, Bryan G. Reuben,[§] and Chava Lifshitz**Department for Physical Chemistry and The Farkas Center for Light Induced Processes, The Hebrew University of Jerusalem, Jerusalem 91904, Israel**Received: October 10, 2000; In Final Form: December 5, 2000*

An electrospray ionization–fast flow technique has been employed to study the reactions of doubly protonated bradykinin and des-Arg⁹-bradykinin with CH₃OD and ND₃, respectively. Deconvolution of the experimental mass spectral data followed by simulation of the kinetic data by solution of differential equations leads to sets of apparent and site-specific rate constants. On a time scale of several milliseconds, bradykinin undergoes with ND₃ three fast H/D exchanges and one slow exchange. Three equivalent exchanges are observed with CH₃OD that are nearly 2 orders of magnitude slower than the ND₃ reactions. Up to six hydrogen exchanges are observed for the reaction of des-Arg⁹-bradykinin with ND₃. The more efficient exchange of des-Arg⁹-bradykinin is accompanied by formation of collisionally stabilized complexes between doubly protonated des-Arg⁹-bradykinin and ND₃ at a He carrier gas pressure of about 0.2 Torr. Multiple-collision activation–collision-induced dissociation of reactant and product ions of the isotope exchange reactions was carried out in front of the sampling nose cone of the analyzer quadrupole mass filter system. The degree of deuterium incorporation into the parent doubly protonated ions and into several of the b_n^+ and y_n^+ ions combined with the site-specific rate constants obtained indicates that the three equivalent hydrogens exchanged in doubly protonated bradykinin are at the protonated N-terminus amine group. Complexation of doubly protonated bradykinin by ND₃ is prevented by its tightly folded structure, and this in turn prevents H/D exchange of the amide hydrogens of bradykinin. The additional H/D exchanges observed in the case of doubly protonated des-Arg⁹-bradykinin are made possible by complexation of its less compact structure via hydrogen-bonded intermediates that promote H/D exchange of amide hydrogens.

Introduction

There has been increasing interest in recent years in anhydrous protein and peptide ions.¹ Conformational properties of biomolecules in solution are said to be preserved during the process of electrospray ionization (ESI) that is used in mass spectrometry (MS) to introduce these biomolecules into the gas phase.² Conformational changes in proteins were probed by hydrogen-exchange electrospray ionization mass spectrometry (ESIMS).^{2,3} The generally held idea has been that compact structures protect some labile hydrogen atoms from H/D exchange in the gas phase. ESI was combined with Fourier transform ion cyclotron resonance (FTICR) spectrometry, and correlations were drawn between specific H/D exchange levels observed in the gas phase and conformations that have been characterized in solution.⁴ H/D exchange was studied for shape-resolved cytochrome *c* conformers preselected through their drift velocities in gas-phase ion mobility experiments.⁵ The interpretation of H/D exchange experiments requires a knowledge of the reaction mechanisms involved. Many studies of H/D exchange between protonated peptides and deuterated solvent molecules were performed.⁶ ND₃ was found to be the most efficient reagent studied for promoting H/D exchange. Other reagents studied include D₂O, CD₃OD,

DI, and CD₃CO₂D. Most of these studies were carried out at very low ion source pressures of 10⁻⁷ to 10⁻⁵ Torr in FTICR mass spectrometers.

We have demonstrated recently⁷ that an electrospray ion source combined with a flow tube reactor can be employed to study ion/molecule reactions of protonated diglycine, GLY₂H⁺, under carrier gas pressures of several tenths of a Torr. We have furthermore observed the formation of collisionally stabilized complexes of GLY₂H⁺ with NH₃, methanol, and a series of amines and studied their formation kinetics. In a study of H/D exchange with ND₃,⁸ we have monitored for the first time the collision complexes corresponding to the consecutive H/D exchanges of the five labile hydrogens in protonated diglycine. The formation kinetics, multi-collision-induced dissociation, and H/D exchange characteristics were studied for the protonated betaine/ammonia complex⁹ that has partial zwitterionic character.¹⁰

The nonapeptide bradykinin, BK (Arg-Pro-Pro-Gly-Phe-Ser-Pro-Phe-Arg or RPPGFSPFR), has attracted considerable attention recently.^{6a,11–28} ESI forms BK in the singly, doubly, and triply protonated states.^{11,12} The gas-phase basicity of protonated BK has been determined by a modified kinetic method.¹³ Collision cross sections deduced from ion chromatography experiments¹⁴ have indicated that BK wraps itself around the charge center(s) in a globular shape. Kinetic energy release distributions determined for charge-separation reactions of doubly protonated BK¹⁶ have indicated that it has a folded rather than an extended geometry and that the conformation is fairly rigid. A strong intramolecular interaction through a proton bridge

[†] Part of the special issue "Edward W. Schlag Festschrift".

* To whom correspondence should be addressed. Phone: (972)-2-6585866. Fax: (972)-2-6522472. E-mail: chavalu@vms.huji.ac.il.

[‡] Permanent address: University Centre for Pharmacy, A. Deusinglaan 1, 9713 AV Groningen, The Netherlands.

[§] Permanent address: School of Applied Science, South Bank University, London SE10AA, England.

between the guanidino groups of the N- and C-terminal arginines of BK was invoked on the basis of post-source-decay product ions.²⁵ BK has been studied by the ion mobility technique,^{14,18} and by BIRD.¹⁵ These studies, combined with calculations by the AMBER suite of programs,¹⁴ have indicated that the lowest energy conformer of singly protonated BK is a salt bridge structure in which the deprotonated carboxylic acid is located between the two protonated arginine residues. Further support for a salt bridge structure as the most stable conformer in the gas phase has come from recent DFT calculations.²⁸ Fragmentations of BK have been studied by, in addition to BIRD, several other slow heating methods including IR heating,²⁴ SORI-CID,²⁷ and thermal dissociation in a quadrupole ion trap.²³ The major reactions of the singly, doubly, and triply protonated BK have been identified and their Arrhenius activation parameters determined.

Several studies of gas-phase H/D exchange of singly, doubly, and triply protonated BK and of several BK derivatives have appeared recently.^{6a,19–22,26} Experiments were carried out at the relatively low pressures of FTICRs and ion traps. A model was developed²⁰ describing the deuterium uptake of an ensemble of $(\text{BK} + \text{H})^+$ gas-phase ions which are exposed to D_2O vapor. The rate and extent of gas-phase H/D exchange of BKs furnished further evidence for the existence of zwitterions (i.e., salt bridge structures) in the gas phase.²² The rate data for $(\text{BK} + 2\text{H})^{2+}$ indicated the presence of at least two noninterconverting ion populations.²¹ It has been demonstrated that H/D exchange kinetics and DI attachment kinetics can be used as chemical probes of three-dimensional gaseous polypeptide ion structures.²¹

A general classification was proposed for H/D exchange mechanisms.^{6a–c} The labile proton at the charge site is intimately involved in the first mechanism. For example, exchange of the three hydrogens on the protonated N-terminus amino group of glycine oligomers with ND_3 as the reagent gas proceeds via an “onium” mechanism in which the endothermicity of proton transfer to ammonia is compensated by intermolecular solvation of the resultant ammonium ion. Protons at the charge site are not directly involved in the second mechanism. An example is the salt bridge mechanism in which proton transfer to a basic exchange reagent leads to a charge-separated ion pair that can be stabilized by favorable interaction with a proximal charge (e.g., the protonated N-terminus). Exchange of carboxylic acid and amide hydrogens in glycine oligomers proceeds via a salt bridge mechanism. These exchange mechanisms have been verified recently by density functional theory calculations.²⁹

In this report we describe our first results on a medium-sized peptide using ESIMS in combination with a fast flow technique. We have chosen BK for this study since, on one hand, so much prior information is available concerning this peptide and, on the other hand, there are still many discrepancies and unknown aspects.

Experimental Section

We constructed a SIFT apparatus some years ago.³⁰ This apparatus has been modified to work with an electrospray ionization source connected directly to the flow tube, as in the work of Poutsma et al.,³¹ and not through the injector quadrupole; reactant ions are thus not mass selected. The system has been described in detail.^{7–9} Briefly, the SIFT consists of a flow reactor that is 123 cm in length with an inner diameter of 74 mm. A neutral reagent is introduced into the flow tube through either one of two ring inlets. Tylan mass flow controllers define the flow rate of the neutral reactant into the flow tube. The quadrupole mass analyzer is housed in a differentially pumped

chamber that is separated from the flow tube by a nose cone (NC) skimmer with a 1.0 mm sampling orifice. In the conventional operation of the apparatus, a small NC voltage is used for focusing ions into the analysis quadrupole. Helium or nitrogen buffer gas enters the flow tube at the upstream end near an electron impact ion source through another Tylan flow controller. It is pumped through the tube by a Roots blower with flow velocities of up to about 9000 cm s^{-1} with typical pressures of a few tenths of a Torr. The present experiments were run at pressures ranging from 0.1 to 0.4 Torr and at reaction times of several milliseconds.

The system has been employed in the study of reactions of protonated diglycine and protonated betaine.^{7–9} It has been upgraded by addition of a new quadrupole mass filter—652601 ABB EXTREL—and power supplies to allow the study of reactions of ions of higher mass to charge ratio, m/z , such as multiprotonated bradykinins.

The electrospray ion source was designed following ref 31. A capillary tube serves as the interface between the electrospray and the helium flow reactor. Stainless steel tubes 15 cm in length with 0.05 cm i.d. are employed. The entire assembly is inserted into the flow tube at a distance of ~ 96 cm from the sampling orifice, 135° to the direction of the helium flow, through an “O”-ring-type vacuum fitting. A capillary tube of 0.05 cm i.d. introduces an air leak into the flow tube with a pressure of 0.07 Torr and a flow rate of 1.3 L/min (STP); these numbers have to be added to the helium pressure and helium flow rate when rate constants are calculated. Ions are electrosprayed ~ 10 mm through ambient air into the grounded capillary tube from a stainless steel syringe needle biased at 4–5 kV dc. Dilute solutions of the analyte of interest in a polar solvent are delivered to the electrospray needle at flow rates of $1.65 \mu\text{L min}^{-1}$ from a 5000 μL syringe mounted onto a model 100 KD Scientific syringe pump.

Second-order rate coefficients are obtained by monitoring the intensity of the primary ion decay as a function of the neutral gas B concentration introduced downstream.

CID can be applied to products of ion/molecule reactions carried out in the flow tube or to ions injected into the flow tube through the ESI source. The sampled ions are dissociated⁹ by increasing the voltage on the NC, following the work by Bohme and co-workers.³² The extent of collisional dissociation of the sampled ions is controlled by the magnitude of the NC voltage (U_{NC}), which can be varied in our experiments from 0 to -80 V. A grid operated at ground potential is placed at the exit of the flow tube. Upon entering the detection region of the apparatus, ions experience sequentially a front-lens voltage ($U_{\text{fl}} = 0$ to -100 V), a quadrupole field (rf/dc), and a channeltron voltage (-2000 to -2500 V). Conversion from laboratory ion energy to the center-of-mass energy frame is possible through multiplication of the nose cone voltage by a mass factor. Nitrogen was employed as the carrier gas in the CID experiments.

BK and des-Arg⁹-BK (dA⁹BK) were samples from Sigma/Aldrich with a stated minimum purity of 98–99%. Dilute solutions of these peptides in 1% acetic acid, 49% water, and 50% methanol were employed to electrospray the protonated peptides. ND_3 was from Sigma/Aldrich with a stated isotopic purity of ≥ 99 atom % D.

Data Analysis

1. Deconvolution of Mass Spectral Data. The elemental formula of doubly protonated BK is $\text{C}_{50}\text{H}_{75}\text{N}_{15}\text{O}_{11}$. The isotopic natural abundance distribution complicates the analysis of the

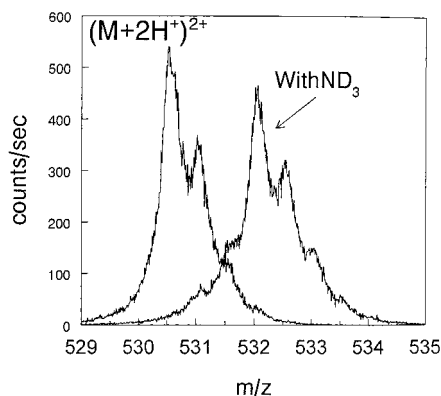


Figure 1. Mass spectra (intensities in ion counts per second vs m/z) of isotopic multiplets of doubly protonated bradykinin. Electrospray ionization is combined with a fast flow technique, and mass analysis is by a quadrupole mass filter. Spectra shown are for the reactant ion and for the product following partial deuterium exchange by ND_3 .

deuterium labeling data. Larger peptides and proteins would present an even bigger problem. Successful interpretation of the experiments requires removal of the isotopic natural abundance distribution to reveal the underlying distribution of artificially introduced deuterium.¹⁷ In FTICRs this can be achieved by ejecting all ions except for one isobar before performing H/D exchange. However, the low relative abundance for any one isobar reduces the feasibility of that approach.¹⁷ The goal can be achieved through isotopic deconvolution. The isotopic multiplet of $(\text{BK} + 2\text{H})^{2+}$ is observed to shift to higher masses (Figure 1) upon introduction of ND_3 into the flow tube. The measured peaks are made up of contributions from undeuterated bradykinin and its mono-, di-, and trideuterio isotopomers (with a small contribution from a tetradeuterio isotopomer). The undeuterated ion and its deuterated isotopomers each contribute a multiplet of overlapping isotopic peaks due to the natural abundances of the various carbon, nitrogen, oxygen, and hydrogen isotopes. Let the abundances of the four major hydrogen/deuterium isotopomers be given by m , $m + 1$, $m + 2$, and $m + 3$. If the peak shape of the multiplet given by the undeuterated isotopomer is $f(m)$, then the peak shapes of the other isotopomers will be $f(m+1)$, $f(m+2)$, and $f(m+3)$. These multiplets will be identical with the undeuterated multiplet but displaced 1, 2, and 3 mass units (or, in the case of doubly charged ions, 0.5, 1, and 1.5 units). The overall peaks as measured will be the sum of these multiplets multiplied by their abundances, that is

$$\sum mf(m) + (m+1)f(m+1) + (m+2)f(m+2) + (m+3)f(m+3) \quad (1)$$

Or, in more general terms

$$\sum_0 (m+n)f(m+n) \quad (2)$$

The function $f(m)$ may be established experimentally from runs at zero flow rate, and the proportions of the deuterated isotopomers contributing to the products of the reaction may be deduced by combining these distributions in different proportions to give the minimum sum of squares deviation from the experimental results.

This is done with the aid of the Microsoft Excel "Solver" program. It uses the generalized reduced gradient (GRG2) nonlinear optimization code³³ and, in this case, optimizes m , m

+ 1, $m + 2$, and $m + 3$ to minimize the squares of the differences between the predicted and measured overall peak patterns.

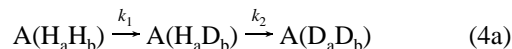
The method has the advantage of minimizing the effects of variations of isotopic ratios in natural products. It minimizes the effects of noise and of asymmetric peak shapes and limitations of resolution in the spectra such as the ones presented in Figure 1.

2. Apparent and Site-Specific Rates. Once the spectra have been deconvoluted, one obtains a set of curves for consecutive deuterium exchanges, as a function of the flow rate of the deuterating agent. Simulation of the kinetic data by solution of the associated set of coupled differential equations yields a set of apparent rate constants; however, it is the set of site-specific rate constants that are of interest.^{6g,j,k,34} An algorithm based on a Modelmaker program of Cherwell Scientific solves a set of independent simultaneous differential equations for a suggested reaction mechanism and is the way for extracting site-specific rate constants that we have adopted.

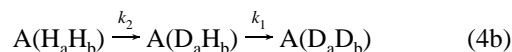
The site-specific rate constants are based on the observation that the kinetics of sequential reactions are different from those for parallel reactions. For sequential reactions involving the replacement of hydrogen by deuterium, one can write^{34b}



where D_0 , D_1 , and D_2 denote molecules containing zero, one, and two deuterium atoms in place of hydrogen atoms, respectively, irrespective of the deuteration site, and the rate constants are k_a and k_b . For parallel reactions of two site-specific reactions, there will be two alternative sequences:



and



The combination of the two reaction sequences will give different kinetics. For example, the apparent first step in the sequential mechanism with an apparent rate constant k_a will be made up of the sum of the two site-specific constants k_1 and k_2 . In the case of exchange of protonated monoglycine with D_2O , there are four site-specific rate constants, three of them identical, corresponding to the exchange of the three equivalent hydrogens of the protonated amine group and a fourth that is different corresponding to the single carboxyl hydrogen of the molecule.^{6g,34b}

He and Marshall³⁴ have used a weighted quasi-Newton algorithm for function minimization and a variable-order, variable-step Adams algorithm for ordinary differential equations to solve site-specific rate constants. Modelmaker 3 solves the simultaneous first-order differential equations corresponding to an assumed mechanism by the Runge–Kutta method. Lebrilla and co-workers^{6g} have used a similar approach. If one sets up a sequence of reactions both parallel and sequential, the program will predict the concentrations of the various intermediates and products if given the appropriate rate constants. Conversely, given experimental data, it will determine the optimum rate constants by one of the standard nonlinear regression methods. The package permits the choice of the Levenberg–Marquardt or Simplex method. The former is generally the method of choice. It corresponds to a minimization of the weighted sum of squares, and if all the weights are set as unity, then it is

equivalent to a least-squares minimization. The Simplex method involves multidimensional minimization, and its main advantage over the Levenberg–Marquardt method is that it is less likely to find local minima. The rate constants that emerged for the glycine/D₂O system were similar to those produced by the He and Marshall program,^{34b} which is evidence that the methods are internally consistent.

Results and Discussion

1. Hydrogen/Deuterium Exchange Experiments. A. Bradykinin. We were able to produce by electrospray ionization and to inject into the flow tube singly, doubly, and triply protonated BK ions. Doubly protonated bradykinin ions (BK + 2H)²⁺ were the most abundant ions under our experimental conditions.

Singly protonated BK ions do not undergo H/D exchange in FTICR experiments with either ND₃^{6a} or D₂O.²² The high proton affinity of the end arginine groups and the compact shape of the zwitterionic structure prevent the exchange from taking place. Earlier reports on H/D exchange with D₂O^{20,35} are now known to be due to quadrupolar axialization in the FTICR experiment to keep the ions centered in the cell. This axialization converted magnetron motion into cyclotron motion and heated the ions enough to produce H/D exchange that would not have occurred at room temperature.³⁶

Doubly protonated BK, (BK + 2H)²⁺, is known to undergo exchange in FTICR experiments with CH₃OD¹⁹ and with D₂O.²² Three hydrogens were exchanged with CH₃OD with similar site-specific rate constants,¹⁹ whereas 16 fast exchanges and 3 slow ones were observed for D₂O over an extended period of 1 h at a relatively high pressure of 1 × 10⁻⁵ Torr.²² We reacted (BK + 2H)²⁺ in the flow tube with either ND₃ or CH₃OD and monitored the incorporation of deuterium as a function of flow rate of the deuterating reagent at a constant reaction time. Some characteristic results are represented in Figures 2–4. The exchange of three labile hydrogens is clearly observed for CH₃OD (Figure 2) in agreement with Green and Lebrilla.¹⁹ There are 19 exchangeable hydrogens in (BK + 2H)²⁺ – 3 at the N-terminus and 10 guanidine (arg¹, arg⁹), 1 hydroxy (ser⁶), and 5 amide hydrogens. The amine end group is protonated in addition to the two arginines in diprotonated BK²² (see Figure 8 of ref 22), leading to three equivalent labile hydrogens at the N-terminus not available in the singly protonated BK. It is these three hydrogens that are proposed to exchange out of the 19 exchangeable hydrogens in (BK + 2H)²⁺. Three labile hydrogens of BK are also observed to exchange in the flow tube experiment with ND₃ (Figure 3). There is evidence for a minor contribution from an additional exchange of a fourth labile hydrogen (Figure 4) that could be due to the hydroxyl group of serine (ser⁶). The C-terminus is deprotonated in the suggested salt bridge structure (Figure 8 of ref 22). If there are two noninterconverting ion populations,²¹ it is possible that one of these undergoes H/D exchange at the C-terminus.

As noted in the Introduction, we were able to monitor the collision complexes corresponding to consecutive H/D exchanges in our previous flow tube reactor study of protonated diglycine.⁸ However, contrary to the case of GLY₂H⁺,⁷ for which we were able to observe the formation of collisionally stabilized complexes with NH₃, analogous complexes of doubly protonated BK with ammonia could not be collisionally stabilized. We did observe the highly efficient formation of collision complexes between (BK + 2H)²⁺ and trimethylamine at a carrier gas pressure of 0.23 Torr (see Figure 5).

When the gas-phase basicities of the deuterating reagent and the substrate undergoing exchange are similar, H/D exchange

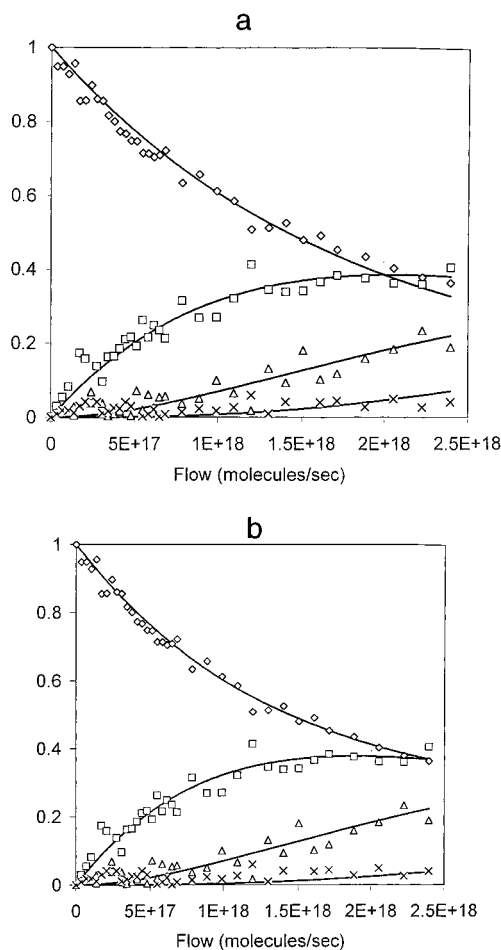


Figure 2. Relative abundance vs flow rate of the neutral deuterating reagent for various cations in the reaction of [BK + 2H]²⁺ with CH₃OD. Symbols are experimental with \diamond , \square , \triangle , and \times representing species in which zero, one, two, and three hydrogens have been replaced by deuterium, respectively. The curves are the simulated fits for derivation of (a) apparent rate constants and (b) site-specific rate constants; see the text.

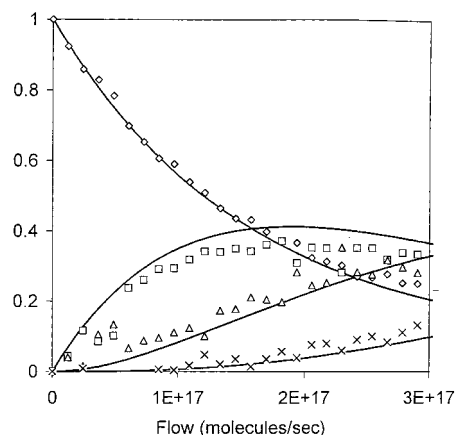


Figure 3. Relative abundance vs flow rate of the neutral deuterating reagent for various cations in the reaction of [BK + 2H]²⁺ with ND₃. Symbols are experimental with \diamond , \square , \triangle , and \times representing species in which zero, one, two, and three hydrogens have been replaced by deuterium, respectively. The curves are the simulated fits for derivation of site-specific rate constants; see the text.

occurs by simple proton transfer possibly through a four-center intermediate.^{6j} However, the gas-phase basicity of protonated bradykinin, 217.8 kcal/mol,¹³ is considerably higher than that of ammonia, 195.6 kcal/mol.³⁷ It is conceivable that a collision

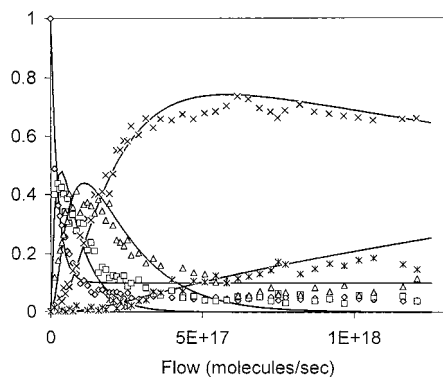


Figure 4. Relative abundance vs flow rate of the neutral deuterating reagent for various cations in the reaction of $[\text{BK} + 2\text{H}^+]^{2+}$ with ND_3 as in Figure 3 but at higher flow rates. Symbols are experimental with \diamond , \square , \triangle , \times , and $*$ representing species in which zero, one, two, three, and four hydrogens have been replaced by deuterium, respectively.

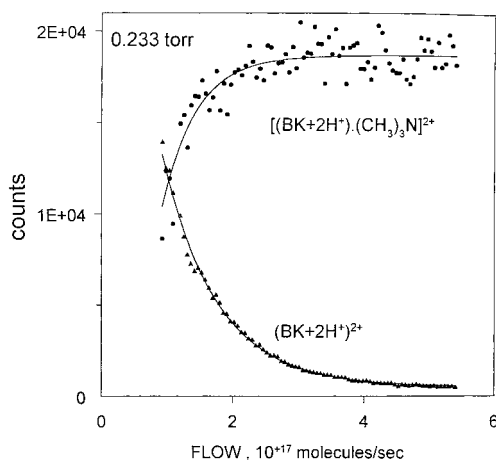


Figure 5. Reactant and product ion intensities in the reaction of $[\text{BK} + 2\text{H}^+]^{2+}$ with trimethylamine, $(\text{CH}_3)_3\text{N}$, at a helium carrier gas pressure of 0.233 Torr. The product is the collisionally stabilized complex between $[\text{BK} + 2\text{H}^+]^{2+}$ and $(\text{CH}_3)_3\text{N}$.

complex with ND_3 is being formed; however, the potential well is too shallow for it to be collisionally stabilized at the pressures existing in the flow tube.

b. Des-Arg⁹-bradykinin. The most stable conformer of the doubly protonated octapeptide, dA^9BK ($\text{R}^+\text{PPGFSPF}^+$), has an extended structure with an interchange distance of 14.3 Å.³⁸ Although its labile hydrogens are exposed in such an open structure, this peptide was found to be very unreactive with CH_3OD , exchanging a single labile hydrogen extremely slowly.¹⁹ We have followed the reaction of $[\text{dA}^9\text{BK} + 2\text{H}^+]^{2+}$ with ND_3 and observed fast H/D exchange. At least five labile hydrogens were observed to undergo exchange with a quite firm indication for a sixth exchange. Each consecutive H/D exchange is accompanied by formation of a collisionally stabilized complex between the corresponding protonated or deuterated dA^9BK and ND_3 . The formation reactions of collision complexes track the H/D exchanges as has been the case for protonated diglycine.⁸ Typical examples of flow tube experimental results are presented in Figure 6. These results confirm the existence of an open exposed structure of $[\text{dA}^9\text{BK} + 2\text{H}^+]^{2+}$ contrary to the compact structure of $[\text{BK} + 2\text{H}^+]^{2+}$. The exposed structure of doubly protonated des-Arg⁹-bradykinin allows the complexation by ammonia through multiply hydrogen-bonded structures that involve the backbone carbonyl groups as in the case for GLY_2H^+ .^{29a} The poor reactivity of CH_3OD with protonated dA^9BK has been ascribed to steric hindrance but is not quite well understood.¹⁹ It is worthwhile contemplating again the reasons

for this poor reactivity, particularly in view of the efficient reaction with ND_3 observed here. The exchange mechanisms for D_2O and CH_3OD on one hand and ND_3 on the other are different. ND_3 is basic enough to gain a proton and be solvated by the peptide, whereas D_2O and CH_3OD are incapable of deprotonating the peptide ion and were postulated to exchange via a “relay mechanism”, in which the reagent simultaneously gains a D while losing an H.^{6b,k}

2. Determination of Apparent and Site-Specific H/D Exchange Rate Constants. The experimental points presented in Figures 2–4 are the ones obtained following isotopic deconvolution (see Data Analysis, subsection 1). The curves are the result of simulation of the kinetic data by solution of the associated set of differential equations (see Data Analysis, subsection 2). The simulation given in Figure 2a corresponds to the apparent rate constants, whereas the ones in Figures 2b, 3, and 4 yield the site-specific rate constants. Overall disappearance rate constants were deduced from semilogarithmic decay plots of the reactant ion. Table 1 summarizes the rate constants obtained.

$[\text{BK} + 2\text{H}^+]^{2+}$ exchanges three hydrogens upon reaction with either ND_3 or CH_3OD . The three site-specific rate constants deduced are equal for CH_3OD (see Table 1). This indicates that the three sites undergoing exchange in doubly protonated bradykinin are equivalent. The set of rate constants obtained for the ND_3 reaction system is more than an order of magnitude larger than for CH_3OD , as is expected in view of the stronger basicity of ND_3 . The three high site-specific rate constants for ND_3 are not equal; in most of the experiments they are made up of two equal rates and a third that is about twice as high as the first two. This may reflect the fact that ND_3 can exchange more than one hydrogen atom per collision with protonated BK whereas CH_3OD cannot. Beauchamp and co-workers^{6a} reported on extensive multiple exchanges for ND_3 . As a result, the apparent rate constants deduced for the reaction of ND_3 with $[\text{BK} + 2\text{H}^+]^{2+}$ (Table 1) may be more significant than the site-specific ones. A fourth hydrogen exchange is observed for the ND_3 reaction at a considerably lower rate than the first three (Table 1), indicating the presence of a separate site of exchange of a single labile hydrogen in bradykinin.

The $[\text{BK} + 2\text{H}^+]^{2+}/\text{ND}_3$ reaction involves a proportion—very close to 10%—of material that does not react. This has been taken into account in the simulations. The rate constant for $[\text{BK} + 2\text{H}^+]^{2+}$ disappearance was estimated from 10 runs as $(1.44 \pm 0.6) \times 10^{-9} \text{ cm}^3 \text{ molecule}^{-1} \text{ s}^{-1}$ (see Table 1) on the assumption of 10% inert material and a measured 2.7% level of protium contamination in the ND_3 . Overall rate constants taking the whole of the initial concentration of BK into account would be about 12% lower.

The existence of two noninterconverting ion populations of $[\text{BK} + 2\text{H}^+]^{2+}$ with different reactivities has been observed before. On the basis of the interaction with HI, it was concluded²¹ that the two populations were present in roughly equal abundance at room temperature, whereas in our experiments we found a ratio of about 1:9. Ion mobility experiments¹⁸ have indicated only one conformation for doubly protonated BK. The explanation for the discrepancies between different experiments regarding the existence and population abundance ratios of the two conformers has to await additional experiments and/or computations.

The ion mobility experiments have shown further¹⁸ that the cross-sections of singly and doubly protonated BK change by only 1 Å². This result demonstrates,¹⁸ in agreement with the charge-separation experiments of doubly protonated BK,¹⁶ that

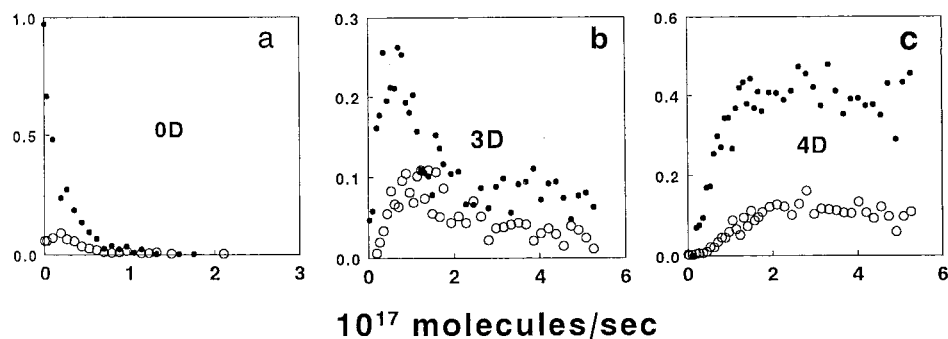


Figure 6. Relative abundance vs flow rate of the neutral deuterating reagent for various cations in the reaction of $[\text{dA}^9\text{BK} + 2\text{H}^+]^{2+}$ with ND_3 . Filled symbols represent uncomplexed ions, whereas open symbols represent ions complexed by ND_3 . Panels a, b, and c represent results for species in which zero, three, and four hydrogens have been replaced by deuterium, respectively.

TABLE 1: Apparent, Site-Specific, and Overall H/D Exchange Rate Constants ($\text{cm}^3 \text{molecule}^{-1} \text{s}^{-1}$) for $(\text{BK} + 2\text{H}^+)^{2+}$ with CH_3OD and ND_3

CH_3OD				ND_3			
k_{apparent}	$k_{\text{site-specific}}$	$\Sigma k_{\text{site-specific}}$	$k_{\text{semilog plot}}$	k_{apparent}	$k_{\text{site-specific}}$	$\Sigma k_{\text{site-specific}}$	$k_{\text{semilog plot}}$
5.0×10^{-11}	1.6×10^{-11}			1.44×10^{-9}	9.2×10^{-10}		
3.3×10^{-11}	1.6×10^{-11}	4.8×10^{-11}	4.3×10^{-11}	7.1×10^{-10}	3.0×10^{-10}	1.53×10^{-9}	1.31×10^{-9}
1.9×10^{-11}	1.6×10^{-11}			3.7×10^{-10}	2.9×10^{-10}		
					1.8×10^{-11}		

$[\text{BK} + 2\text{H}^+]^{2+}$ is just as compact as $[\text{BK} + \text{H}^+]^{1+}$. The only difference is the additional protonation of the amine group in $[\text{BK} + 2\text{H}^+]^{2+}$. Our observation of three major equivalent exchanges for both ND_3 and CH_3OD is thus understandable. The result for CH_3OD is in agreement with Green and Lebrilla,¹⁹ although we observe considerably higher rate constants. It is surprising that the FTICR experiment with D_2O has demonstrated²² 16 fast exchanges and 3 slow ones for $[\text{BK} + 2\text{H}^+]^{2+}$ and no exchange with $[\text{BK} + \text{H}^+]^{1+}$ whereas the flow tube experiment with ND_3 gives only 3 major exchanges and 1 minor one for $[\text{BK} + 2\text{H}^+]^{2+}$. This can be explained as follows: A simplified calculation indicates that an ion undergoes about 1×10^6 collisions with the deuterating reagent in the FTICR experiment for 1 h at a pressure of 10^{-5} Torr²² and about 4000 collisions during 13 min at 10^{-7} Torr.¹⁹ However, there are only about 70 collisions in the flow tube experiment over a period of several milliseconds at a deuterating reagent flow velocity of 1.2×10^{18} molecules/s. This prevents observation in the flow tube of many consecutive exchanges. In addition the FTICR experiments may involve internally hot ions, whereas the flow tube experiments are truly thermal. We have carried out a single run with a flow tube heated to 40 C. This gave an overall rate constant of $7.0 \times 10^{-9} \text{cm}^3 \text{molecule}^{-1} \text{s}^{-1}$ with ND_3 , a high value substantially outside the error limits for the rate in the unheated system. It led also to an increased degree of the fourth H/D exchange.

3. Multiple-Collision Activation—Collision-Induced Dissociation (MCA—CID). We have performed MCA—CID experiments in front of the sampling nose cone of the analyzer quadrupole mass filter on doubly protonated BK and dA^9BK . The results are represented in Figures 7 and 8, respectively. $[\text{BK} + 2\text{H}^+]^{2+}$ produces the well-known fragments observed earlier under thermal dissociation²³ and BIRD¹⁵ experiments. These include the y_7^+ and y_6^+ fragments (nomenclature of Roepstorff³⁹) from the carboxyl end of the peptide, the b_2^+ fragment from the amine end, and a water loss peak from the doubly charged ion. In addition we observe further fragmentation leading to structurally informative y and b fragments (see Figure 7). y ions are protonated peptides that are formed by cleavage of the peptide bond and transfer of two hydrogens from the amine end of the molecule. b ions contain the original amine

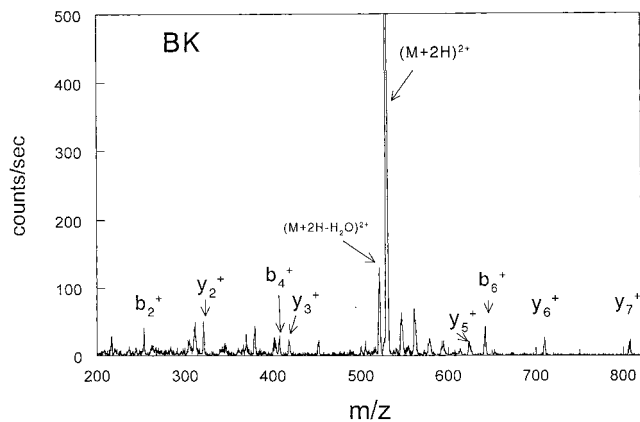


Figure 7. A mass spectrum of doubly protonated BK obtained following MCA—CID in front of the sampling nose cone of the analyzer quadrupole mass filter.

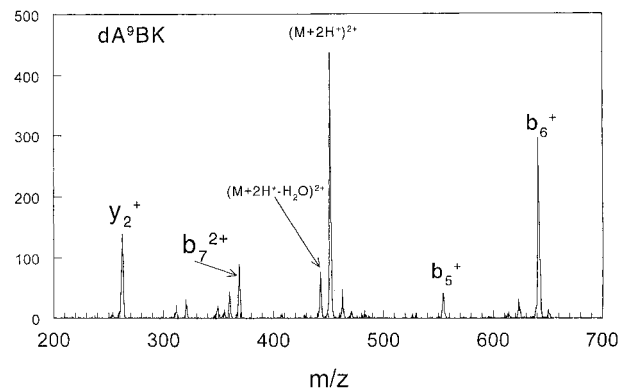


Figure 8. A mass spectrum of doubly protonated dA^9BK obtained following MCA—CID in front of the sampling nose cone of the analyzer quadrupole mass filter.

group of the peptide. MCA—CID of $[\text{dA}^9\text{BK} + 2\text{H}^+]^{2+}$ produces (see Figure 8) the ions b_6^+ , b_5^+ , and b_7^{2+} that have been reported previously³⁹ on the basis of MIKE (mass-analyzed ion kinetic energy) spectroscopy. Additional ions observed are the water loss peak from the doubly charged ion and various y ions, particularly y_2^+ .

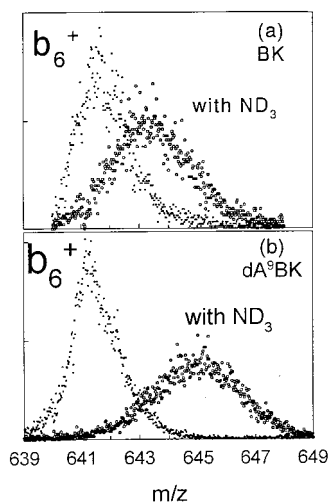


Figure 9. Shift of the m/z of b_6^+ ions upon deuteration at high ND_3 flow rates ($\sim 6 \times 10^{18}$ molecules/s): (a) for BK; (b) for dA^9BK .

According to the *mobile proton model*,⁴⁰ the proton added to the peptide does not remain fixed at the site of greatest proton affinity but is capable of migrating to positions of lower proton affinity prior to fragmentation. This can lead to extensive H/D scrambling prior to collisionally activated dissociation of partially deuterated peptides.⁴¹ The critical energy for H^+ migration may exceed the critical energy for fragmentation in the case of arginine-containing peptides because of the high proton affinity of arginine.⁴¹ However, the proton at the amine end of doubly protonated BK is probably mobile. Any conclusion concerning the deuteration site based on MCA-CID data is therefore tentative. We have measured the shifts in mass upon deuteration with ND_3 of various peaks in the CID spectrum. The water eliminated from deuterated BK does not contain deuterium. Its formation mechanism is not quite clear.²³ The ions y_6^+ and y_7^+ from BK shift upward by three mass units. The ion b_6^+ from BK shifts upward by two mass units, whereas b_6^+ from dA^9BK shifts upward by four mass units (Figure 9). The present results for the mass shifts of b and y ions from BK indicate that the amine end is exchanged upon deuteration of BK, in agreement with the site-specific rate measurements. The additional deuteration of the b_6^+ ion observed in dA^9BK beyond that observed for b_6^+ in BK is ascribed to exchange of amide hydrogens. This exchange becomes possible in dA^9BK due to complexation and hydrogen bonding to the carbonyl groups that is in turn not possible in the case of the tightly folded BK.

Conclusions

An electrospray ionization-flow tube experiment has been applied to the study of H/D exchange of the nonapeptide BK and of dA^9BK . This has demonstrated for the first time the capability of such a system in the study of medium-sized peptides. It opens up the possibility of determining truly thermal rate constants. The relatively high carrier gas pressure allows the observation of collisional stabilization of chemically activated complexes between protonated peptides and small non-covalently bound molecules. A correlation has been observed between the tendency for H/D exchange of backbone amide hydrogens and the ability to form such collision complexes with the deuterating molecules, e.g., ND_3 . Tightly folded peptides such as doubly protonated bradykinin do not form long-lived collision complexes and do not exchange the amide hydrogens. Open structures having a "randomly" located proton such as doubly protonated des-Arg⁹-bradykinin⁴⁰ form long-lived com-

plexes that can be collisionally stabilized, and these structures undergo H/D exchange at backbone amide sites.

Acknowledgment. We thank Drs. Marshall, Bowers, Wesdemiotis, and Hansel for helpful discussions. B.G.R. thanks The Royal Society for a study grant.

References and Notes

- (1) Hoaglund-Hyzer, C. S.; Counterman, A. E.; Clemmer, D. E. *Chem. Rev.* **1999**, *99*, 3037.
- (2) Wang, F.; Freitas, M. A.; Sykes, B. D.; Marshall, A. G. *Int. J. Mass Spectrom.* **1999**, *192*, 319.
- (3) Katta, V.; Chait, B. T. *Rapid Commun. Mass Spectrom.* **1991**, *5*, 214.
- (4) Suckau, D.; Shi, Y.; Beu, S. C.; Senko, M. W.; Quinn, J. P.; Wampler, F. M., III; McLafferty, F. W. *Proc. Natl. Acad. Sci. U.S.A.* **1993**, *90*, 790.
- (5) Valentine, S. J.; Clemmer, D. E. *J. Am. Chem. Soc.* **1997**, *119*, 3558.
- (6) (a) Campbell, S.; Rodgers, M. T.; Marzluff, E. M.; Beauchamp, J. L. *J. Am. Chem. Soc.* **1994**, *116*, 9765. (b) Campbell, S.; Rodgers, M. T.; Marzluff, E. M.; Beauchamp, J. L. *J. Am. Chem. Soc.* **1995**, *117*, 12840. (c) Lee, S.-W.; Lee, H.-N.; Kim, H. S.; Beauchamp, J. L. *J. Am. Chem. Soc.* **1998**, *120*, 5800. (d) Cheng, X.; Fenselau, C. *Int. J. Mass Spectrom. Ion Processes* **1992**, *122*, 109. (e) Gur, E. H.; de Koning, L. J.; Nibbering, N. M. M. *J. Am. Soc. Mass Spectrom.* **1995**, *6*, 466. (f) Gur, E. H.; de Koning, L. J.; Nibbering, N. M. M. *J. Mass Spectrom.* **1996**, *31*, 325. (g) Gard, E.; Willard, D.; Bregar, J.; Green, M. K.; Lebrilla, C. B. *Org. Mass Spectrom.* **1993**, *28*, 1632. (h) Gard, E.; Green, M. K.; Bregar, J.; Lebrilla, C. B. *J. Am. Soc. Mass Spectrom.* **1994**, *5*, 623. (i) Green, M. K.; Gard, E.; Bregar, J.; Lebrilla, C. B. *J. Mass Spectrom.* **1995**, *30*, 1103. (j) Green, M. K.; Penn, S. G.; Lebrilla, C. B. *J. Am. Soc. Mass Spectrom.* **1995**, *6*, 1247. (k) Green, M. K.; Lebrilla, C. B. *Mass Spectrom. Rev.* **1997**, *16*, 53. (l) Dookeran, N. D.; Harrison, A. G. *J. Mass Spectrom.* **1995**, *30*, 666. (m) Zhang, X.; Ewing, N. P.; Cassady, C. J. *Int. J. Mass Spectrom. Ion Processes* **1998**, *175*, 159. (n) Cassady, C. J. *J. Am. Soc. Mass Spectrom.* **1998**, *9*, 716.
- (7) Koster, G.; Soskin, M.; Peres, M.; Lifshitz, C. *Int. J. Mass Spectrom.* **1998**, *179/180*, 165.
- (8) Koster, G.; Lifshitz, C. *Int. J. Mass Spectrom.* **1999**, *182/183*, 213.
- (9) Koster, G.; Lifshitz, C. *Int. J. Mass Spectrom.* **2000**, *195/196*, 11.
- (10) Zhu, C.; Lifshitz, C. *Chem. Phys. Lett.* **2000**, *320*, 513.
- (11) Wang, G.; Cole, R. B. *Org. Mass Spectrom.* **1994**, *29*, 419.
- (12) Schnier, P. D.; Gross, D. S.; Williams, E. R. *J. Am. Soc. Mass Spectrom.* **1995**, *6*, 1086.
- (13) Kaltashov, I. A.; Fabris, D.; Fenselau, C. C. *J. Phys. Chem.* **1995**, *99*, 10046.
- (14) Wyttenbach, T.; von Helden, G.; Bowers, M. T. *J. Am. Chem. Soc.* **1996**, *118*, 8355.
- (15) Schnier, P. D.; Price, W. D.; Jockusch, R. A.; Williams, E. R. *J. Am. Chem. Soc.* **1996**, *118*, 7178.
- (16) Szilágyi, Z.; Drahos, L.; Vékey, K. *J. Mass Spectrom.* **1997**, *32*, 689.
- (17) Zhang, Z.; Guan, S.; Marshall, A. G. *J. Am. Soc. Mass Spectrom.* **1997**, *8*, 659.
- (18) Countermann, A. E.; Valentine, S. J.; Srebalus, C. A.; Henderson, S. C.; Hoaglund, C. S.; Clemmer, D. E. *J. Am. Soc. Mass Spectrom.* **1998**, *9*, 743.
- (19) Green, M. K.; Lebrilla, C. B. *Int. J. Mass Spectrom. Ion Processes* **1998**, *175*, 15.
- (20) Wyttenbach, T.; Bowers, M. T. *J. Am. Soc. Mass Spectrom.* **1999**, *10*, 9.
- (21) Schaaff, T. G.; Stephenson, J. L., Jr.; McLuckey, S. A. *J. Am. Chem. Soc.* **1999**, *121*, 8907.
- (22) Freitas, M. A.; Marshall, A. G. *Int. J. Mass Spectrom.* **1999**, *182/183*, 221.
- (23) Butcher, D. J.; Asano, K. G.; Goeringer, D. E.; McLuckey, S. A. *J. Phys. Chem. A* **1999**, *103*, 8664.
- (24) Freitas, M. A.; Hendrickson, C. L.; Marshall, A. G. *Rapid Commun. Mass Spectrom.* **1999**, *13*, 1639. Freitas, M. A.; Hendrickson, C. L.; Marshall, A. G. *J. Am. Chem. Soc.* **2000**, *122*, 7768.
- (25) Gimón-Kinsel, M. E.; Barbacci, D. C.; Russell, D. H. *J. Mass Spectrom.* **1999**, *34*, 124.
- (26) Schaaff, T. G.; Stephenson, J. L., Jr.; McLuckey, S. A. *J. Am. Soc. Mass Spectrom.* **1999**, *11*, 167.
- (27) Schnier, P. D.; Jurchen, J. C.; Williams, E. R. *J. Phys. Chem. B* **1999**, *103*, 737.
- (28) Strittmatter, E. F.; Williams, E. R. *J. Phys. Chem. A* **2000**, *104*, 6069.

- (29) (a) Zhu, C.; Balta, B.; Aviyente, V.; Lifshitz, C. *J. Phys. Chem. A* **2000**, *104*, 7061. (b) Balta, B.; Basma, M.; Aviyente, V.; Zhu, C.; Lifshitz, C. *Int. J. Mass Spectrom.* **2000**, *201*, 69.
- (30) Iraqi, M.; Petrank, A.; Peres, M.; Lifshitz, C. *Int. J. Mass Spectrom. Ion Processes* **1990**, *100*, 679.
- (31) Poutsma, J. D.; Seburg, R. A.; Chyall, L. J.; Sunderlin, L. S.; Hill, B. T.; Hu, J.; Squires, R. R. *Rapid Commun. Mass Spectrom.* **1997**, *11*, 489.
- (32) (a) Baranov, V.; Petrie, S.; Bohme, D. K. *J. Am. Chem. Soc.* **1996**, *118*, 4500. (b) Baranov, V.; Bohme, D. K. *Int. J. Mass Spectrom. Ion Processes* **1996**, *154*, 71.
- (33) Lasdon, L.; Waren, A. *Microsoft Knowledge Base XL: Solver* uses the generalized reduced gradient algorithm (Q82890).
- (34) (a) He, F.; Marshall, A. G.; Freitas, M. A. Assignment of Gas-Phase Dipeptide Amide Hydrogen Exchange Rate Constants by Site-Specific

- Substitution: GlyGly. *J. Phys. Chem. A*, submitted for publication. (b) He, F.; Marshall, A. G. *J. Phys. Chem. A* **2000**, *104*, 562.
- (35) Zhang, Z.; Li, W.; Guan, S.; Marshall, A. G. *Proceedings of the 44th ASMS Conference on Mass Spectrometry and Allied Topics*, Portland, OR, 1996; p 1061.
- (36) Marshall, A. G. Private communication, August 2000.
- (37) Lias, S. G.; Liebman, J. F.; Levin, R. D. *J. Phys. Chem. Ref. Data* **1984**, *13*, 695.
- (38) Kaltashov, I. A.; Fenselau, C. C. *J. Am. Chem. Soc.* **1995**, *117*, 9906.
- (39) Roepstorff, P.; Fohlman, J. *J. Biomed. Mass Spectrom.* **1984**, *11*, 601.
- (40) Dongré, A. R.; Jones, J. L.; Somogyi, Á.; Wysocki, V. H. *J. Am. Chem. Soc.* **1996**, *118*, 8365.
- (41) Harrison, A. G.; Yalcin, T. *Int. J. Mass Spectrom.* **1997**, *165/166*, 339.